Applied Surface Science 256 (2010) 5918–5923

Contents lists available at ScienceDirect

Applied Surface Science

journal homepage: www.elsevier.com/locate/apsusc

Sinterability studies on $K_{0.5}Na_{0.5}NbO_3$ using laser as energy source

Xiaoyong Tian[a,b,*], Anne Dittmar[b], Jörg Melcher[c], Jürgen G. Heinrich[b]

[a] State Key Laboratory of Mechanical Manufacture System Engineering, Xi'an Jiaotong University, Xi'an 710049, China
[b] Department for Engineering Ceramics, Clausthal University of Technology, Clausthal-Zellerfeld 38678, Germany
[c] Institute of Composite Structures and Adaptive Systems, German Aerospace Center, Braunschweig 38108, Germany

ARTICLE INFO

Article history:
Received 7 September 2009
Received in revised form 15 March 2010
Accepted 16 March 2010
Available online 23 March 2010

Keywords:
Laser sintering
Piezoelectric ceramics
Texture engineering
Surface treatment

ABSTRACT

The sinterability of $K_{0.5}Na_{0.5}NbO_3$ (KNN) ceramics by a laser beam has been investigated in the present research. A 100 W CO_2 laser with a beam diameter of 0.6 mm has been used to sinter the KNN specimens prepared on a uniaxial pressing machine. The relations between laser power and thickness of densified layer, crystallographic structures and phase compositions have been studied. A comparison has been made between laser and furnace sintered KNN samples according to the SEM, XRD and XRF results. The possibility of KNN used for the layer-wise laser direct sintering 3D components has been confirmed in this paper.

1. Introduction

Lead-free piezoelectric ceramics have gained popularity over lead-based ceramics owing to environmental concerns. $K_{0.5}Na_{0.5}NbO_3$ (KNN) ceramic is a promising candidate material for the lead-free piezoelectric ceramics because of its environment friendly properties and good piezoelectric properties [1]. However, fabrication of KNN ceramic samples using conventional atmospheric sintering process which always being characterized by long soaking period is very difficult because of the high volatility of alkali metal oxide [2,3]. Considerable researches have been focused on the improvement of piezoelectric properties by increasing the densification degree of KNN samples. Some researchers investigated the different sintering processes. Jaeger and Egerton used the hot pressing process to prepare potassium-sodium niobates with relative densities greater than 99% [3]. Spark plasma sintering has been used by Li et al. [4] to produce dense KNN ceramic samples (relative density > 99%) at a low sintering temperature (920 °C). At the same time there are many researchers working on the traditional furnace sintering studies of KNN doped with other elements, including Li, Sb, Ta, Ti, Ca, Ba, Sr, etc. [5–8], to establish KNN based piezoelectric ceramic families with high density and properties. Recently, KNN thin and thick films have been investigated by using pulsed laser deposition [9,10], RF magnetron sputtering [11,12], chemical solution deposition [13] and aerosol deposition [14]. All of these researches have been focused on the development of KNN films with dense microstructures and high piezoelectric properties and their applications in MEMS. Texture engineering has also been introduced to the piezoelectric ceramics preparation process to enhance the physical properties recently [1,15–17]. Higher piezoelectric constant ratio (d_{33}/d_{31}) of KNN based ceramics has been already achieved and indicates that greater anisotropy in properties are related to the anisometric crystallographic structures. Laser as a clean energy source has been more and more widely used to modify the refractory ceramics, ZrC [18], BN, SiC, Si_3N_4 [19], Al_2O_3 [20–23], etc. and to improve the physical properties of functional ceramics, $0.94(K_{0.5}N_{0.5})NbO_3$–$0.06LiTaO_3$ [24], Ta_2O_5 [25], $Bi_4Ti_3O_{12}$ [26], due to the unique microstructures developed from the rapid heating and cooling rate of the laser material processing.

In the present research, the ultimate goal is to produce 3D ceramic components, such as actuators and sensors, by using KNN slurry as starting material and layer-wise laser direct sintering as the fabrication process. Before this, the laser sinterability of KNN ceramic should be investigated. In this paper, KNN powder with a stoichiometry of $K_{0.5}N_{0.5}NbO_3$ was prepared by using conventional calcination process with metal oxide and carbonate. KNN samples were prepared by uniaxial pressing from the powder instead of the KNN slurry due to the similar density with tape casting. And then the pressed KNN specimens were sintered by using laser as the heat source. The influence of laser process parameters on the crystallographic structures and phase compositions has been studied. By comparing the microstructures and phase composition of laser and furnace sintered KNN samples, the sinterability of KNN for the layer-wise laser direct sintering has been confirmed.

* Corresponding author at: Technische Universität Clausthal, Institut für Nichtmetallische Werkstoffe, Zehntnerstrasse 2a, Clausthal-Zellerfeld 38678, Germany. Tel.: +49 5323 723711; fax: +49 5323 723119.
E-mail addresses: leoxyt@hotmail.com, xiaoyong.tian@tu-clausthal.de (X. Tian).

0169-4332/$ – see front matter © 2010 Elsevier B.V. All rights reserved.
doi:10.1016/j.apsusc.2010.03.074

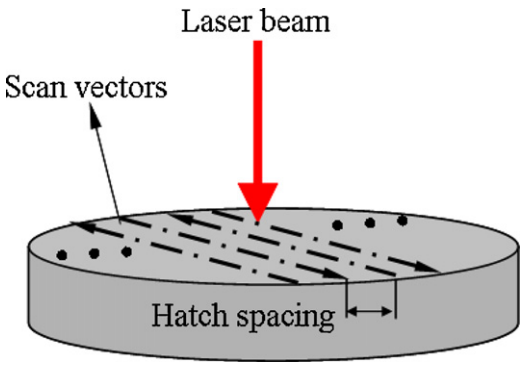

Fig. 1. Laser sintering process on the surface of KNN specimens (preheated to 500 °C) with a hatch spacing of 0.1 mm, and a laser beam diameter of 0.6 mm for the scan vectors (schematic).

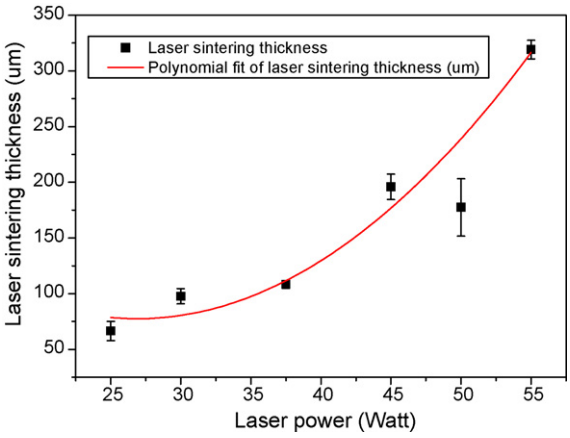

Fig. 2. Relationship between laser power and the thickness of laser sintered layer, with a constant scan speed of 100 mm/s and hatch spacing of 0.1 mm.

The advantages of the laser sintering process, such as controlling the microstructures and modifying the properties, have also been illustrated in present paper. Further measurements of physical properties of laser sintered KNN samples are underway and the results will be published soon.

2. Experimental procedure

The KNN powder was prepared by a conventional ceramic fabrication technique using analytical grade metal oxides and carbonate powders, K_2CO_3 (>99.0%, Sigma–Aldrich, Germany), Na_2CO_3 (>99.8%, Sigma–Aldrich, Germany) and Nb_2O_5 (>99.99%, H.C. Starck, Germany) as the raw materials. All raw materials were weighted in order to obtain a $K_{0.5}Na_{0.5}NbO_3$ ceramic, mixed by ball milling in a PET bottle for 24 h with alumina balls in deionized water, dried and calcinated at 900 °C for 5 h in alumina crucibles. The calcinated powder was ground by disk milling into a fine powder with a mean particle size of 1.866 μm. Then the KNN powder was pressed into pellets with a diameter of 20 mm and weight of 2 g for each specimen on the uniaxial pressing machine under a pressure of 200 MPa. Laser direct sintering was conducted on the pellets using a 100 W CO_2 laser with a beam diameter of 0.6 mm (Rofin Sinar SC10, Hamburg, Germany). Different laser power (from 25 W to 55 W) had been used to investigate its influence on the microstructure and phase composition. The scan speed and hatch spacing were kept as constant values, 100 mm/s and 0.1 mm, in these experiments. The schematic diagram of this sintering process is shown in Fig. 1. Before laser sintering all the samples were put into the cavity of the work-table which were preheated to 500 °C and held for 60 min in order to decrease the thermal stresses produced in the laser sintering process and to reduce the cracks around the interfaces [27]. Some of the pellets were sintered at 1060 °C for 2 h in a furnace to compare the microstructure and phase composition with the laser sintered samples. The microstructures of the fractured cross-section were studied by means of scanning electron microscopy (SEM, CamScan CS4 Cambridge, UK). Crystal phase's identification was performed by X-ray diffraction (XRD, Siemens diffractmeter D 5000, Siemens AG, Germany). Chemical composition was detected by the X-ray fluorescence (XRF).

3. Results and discussion

3.1. Thickness of the laser sintered layer

The relationship between laser power and thickness of laser sintered layers is illustrated in Fig. 2. The thickness of laser sintered layers was measured by SEM on the fresh fractured cross-sections in the laser treated KNN samples, as shown in Fig. 3. The average thickness of laser sintered layers increased with increasing laser power. According to previous research results [27,28], the sintering temperature in the heat affected zone (HAZ) held a direct ratio to the laser energy density. Laser energy density can be calculated by using the following formula:

$$\text{Laser ED} = \frac{P}{D \times V} (\text{J/cm}^2) \quad (1)$$

where P is the laser power, D is the diameter of the laser spot (0.6 mm in present work) and V is the laser scan speed (100 mm/s). When D and V are constant the laser energy density is direct proportional to the laser power. Therefore, with a high sintering temperature, the thickness of laser sintered layer normally achieved a large value. The optimal laser sintering power as well as the sintering temperature was selected according to its influence not only on the thickness of laser sintered layer but also on the microstructure and phase composition, because volatilization of alkali metal oxides happened during the laser sintering process. Microstructure and phase composition have a significant influence on the piezoelectric properties of the final ceramic components. The relationship between laser power and piezoelectric properties has to be investigated to select proper laser sintering parameters. This part of work is still in process right now.

3.2. Microstructure

The surface morphology of laser sintered KNN is shown in Fig. 3. The hatch spacing of 0.1 mm produced parallel linear structures, which can be observed easily on the SEM micrographs in the left column of Fig. 3. The laser spot size of 0.6 mm and hatch spacing of 0.1 mm caused overlapping regions between adjacent scan vectors. In the overlapped areas, double even triple sintering produced crystal inhomogeneous growth and finally induced the heterogeneous microstructures in the laser sintered surface, as shown in Fig. 3a. The laser sintered surfaces with different laser power all exhibited cubical grains. The grains grew bigger and bigger with an increasing laser power equivalent to an increasing sintering temperature from a to d in Fig. 3. In Fig. 3a, cubical grains grew out of the powder matrix because only the areas with multi-sintering had a higher temperature enough to crystallize into cubical grains. The size of produced cubical grains was around 10 μm. In Fig. 3b, more cubical grains grew up in the laser sintered surface. No more powder matrix was observed at this laser energy level. The cubical grains with a size of 10–20 μm stacked together firmly on the surface just like bricks and no cracks appeared between grains. The boundaries between grains were not obvious probably due to the possible liquid sintering process and rapid heating–cooling process

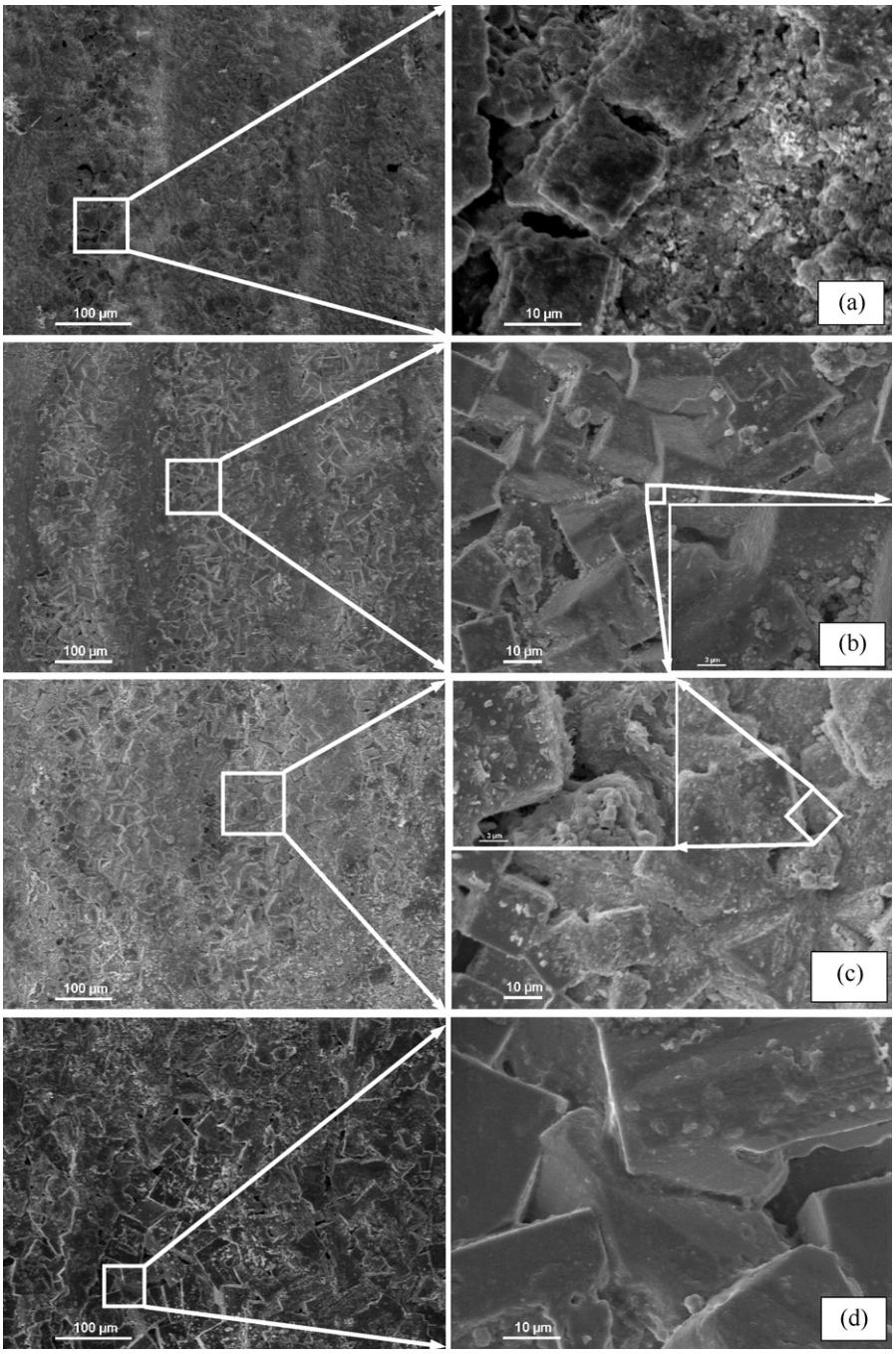

Fig. 3. Surface microstructure development of KNN samples prepared by laser direct sintering with laser power: (a) 25 W, (b) 37.5 W, (c) 45 W, and (d) 55 W; constant scan speed of 100 mm/s and hatch spacing of 0.1 mm.

comparing with the conventional furnace sintering. Liquid phase between adjacent cubical grains has been used to interpret the densification process of KNN ceramics by many researchers [29]. As continue increasing the laser power to 45 W, the grain size had no obvious enlargement. However, the grains surfaces became coarser and some needle-like microstructures appeared on the surfaces of cubic grains, as shown in Fig. 3c and the inset picture. The coarse and need-like microstructures probably caused by the volatilization of alkali metal oxide on the grain surface due to the higher laser power as well as a higher laser sintering temperature. With further increasing the laser power to 55 W the grain size enlarged to around 50 μm and the morphology of the grains changed from the cubic to irregular shape. The coarse and needle-like microstructures disappeared as shown in Fig. 3d. By comparison with Fig. 3c which had a lower laser power of 45 W, the grain size enlargement in Fig. 3d could be explained by the dual actions, volatilization of alkali metal oxide and re-crystallization of the cubical grains under the condition of ultrahigh laser power and sintering temperature.

To compare the microstructure of laser sintered and furnace sintered samples, the SEM micrographs of uniaxial pressed compact KNN powder and furnace sintered samples are shown in Fig. 4. There were some pores in the cross-section of pressed compact KNN powder which had a mean size of 1.866 μm, as shown in Fig. 4a. After furnace sintering at 1060 °C for 2 h, cubic grains had been attained. In the cross-section of furnace sintered sample (Fig. 4b), bigger cubical grains are surrounded by the smaller ones probably caused by the inhomogeneous particle size distribution in the starting powder (Fig. 4a). The boundaries of the cubical grains

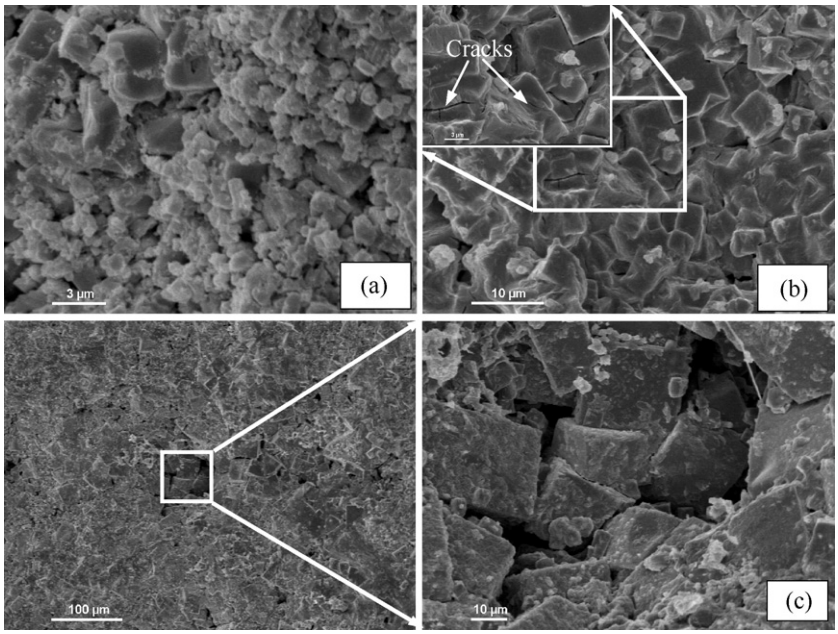

Fig. 4. Microstructure development of KNN samples prepared by (a) pressing at 200 MPa on an uniaxial machine (fractured cross-section); furnace sintered at 1060 °C for 2 h, (b) fractured cross-section, and (c) surface.

were indistinct. There were lots of transgranular cracks in the cross-section, as shown in Fig. 4b. Cubic grains had also been observed on the surface of furnace sintered sample (Fig. 4c). Pores appeared on the surface and probably induced the low density of the KNN samples sintered in the furnace. The morphologies of laser sintered and furnace sintered KNN samples were comparable according to the micrographs in Figs. 3 and 4 except that laser-sintered samples had more dense and crack free microstructures than furnace sintered samples, which can also be confirmed by the micrographs of cross-sections in the laser-sintered samples, as shown in Fig. 5 corresponding to the surface micrographs in Fig. 3. The interfaces between laser sintered layer and powder matrix were distinct. But there were no cracks being observed in the interfacial region after the laser sintering process. Preheating the KNN samples to 500 °C before the laser sintering was important to avoid the cracks. Compared with the powder matrix, the laser sintered layer was dense and almost pore free. Using laser as the heat source, the controllable morphologies and dense pore free sintered layers can be achieved. By controlling the morphology and thickness, the piezoelectric properties of KNN samples could be finally tailored according to the requirements in the future research work. Integrating this into the laser direct sintering process using layer-wise slurry deposition [28], 3D KNN piezoelectric ceramic components could be produced, which possessed the tailored or customized properties.

$0.94(K_{0.5}N_{0.5})NbO_3$–$0.06LiTaO_3$ had also been laser sintered to modify the microstructures and improve the piezoelectric properties by Ji et al. [24]. A mixture of anisometric need like grains of several micrometers in diameter with whisker like grains of several tens of nanometers in diameter had been achieved. These needle-like microstructures were not observed in the present research probably due to the doping of $LiTiO_3$ and the different heating strategies in Ji's research. But according to XRD results, sort of textured orientation structures in the laser sintered surface were attained in both researches.

3.3. Phase and chemical composition

The phase compositions of these KNN samples prepared by different processes were verified by the XRD analysis, as shown in Fig. 6. The phase compositions of the starting powder and furnace sintered KNN samples were consistent with current research results [4,30–33]. The XRD results of the laser-sintered samples show that pure perovskite phase was produced by the laser surface sintering process. When the laser power increased to 55 W, the maximum value of laser power in the present research, the diffraction angle of {0 0 1} peak shifted to a smaller value. It was probably because the high laser power caused a distortion of crystal structure as well as the change of the lattice constants.

From the XRD results shown in Fig. 6, the {0 0 1} diffraction peaks of the laser-sintered samples became predominant comparing with the starting powder and furnace sintered sample, which proved that textured structures appeared in the laser sintered KNN samples. High heating and cooling rate in the laser sintering process might induce a distinct temperature gradient from the laser incidence surface to the inner region of the laser affected area. This temperature gradient finally caused directional growth of the KNN crystals along the {0 0 1} planes. Several methods are available to evaluate the degree of orientation quantitatively [34], but the Lotgering method using XRD is widely used because of its simplicity. In this method, the relative intensity of the diffraction lines, which are related to the textured direction, is used to determine the degree of orientation. The Lotgering F value of the {0 0 1} diffraction peak can be determined using the following formulas [15]:

$$F = \frac{P - P_0}{1 - P_0} \tag{2}$$

$$P = \frac{\sum I_{(0\,0\,1)}}{\sum I_{(h\,k\,l)}} \tag{3}$$

$$P_0 = \frac{\sum I_{0(0\,0\,1)}}{\sum I_{0(h\,k\,l)}} \tag{4}$$

where I and I_0 are the intensity of the diffraction line of the textured and randomly oriented specimens, respectively, and (0 0 1) and (h k l) are the Miller indexes. The orientation degrees (F values) of each sample were shown in Fig. 6 using starting powder as the randomly oriented specimen, which had an F value of zero. Furnace sintered specimen held an F value of 2.52% that was very close to the starting powder, a randomly oriented specimen. Laser-sintered

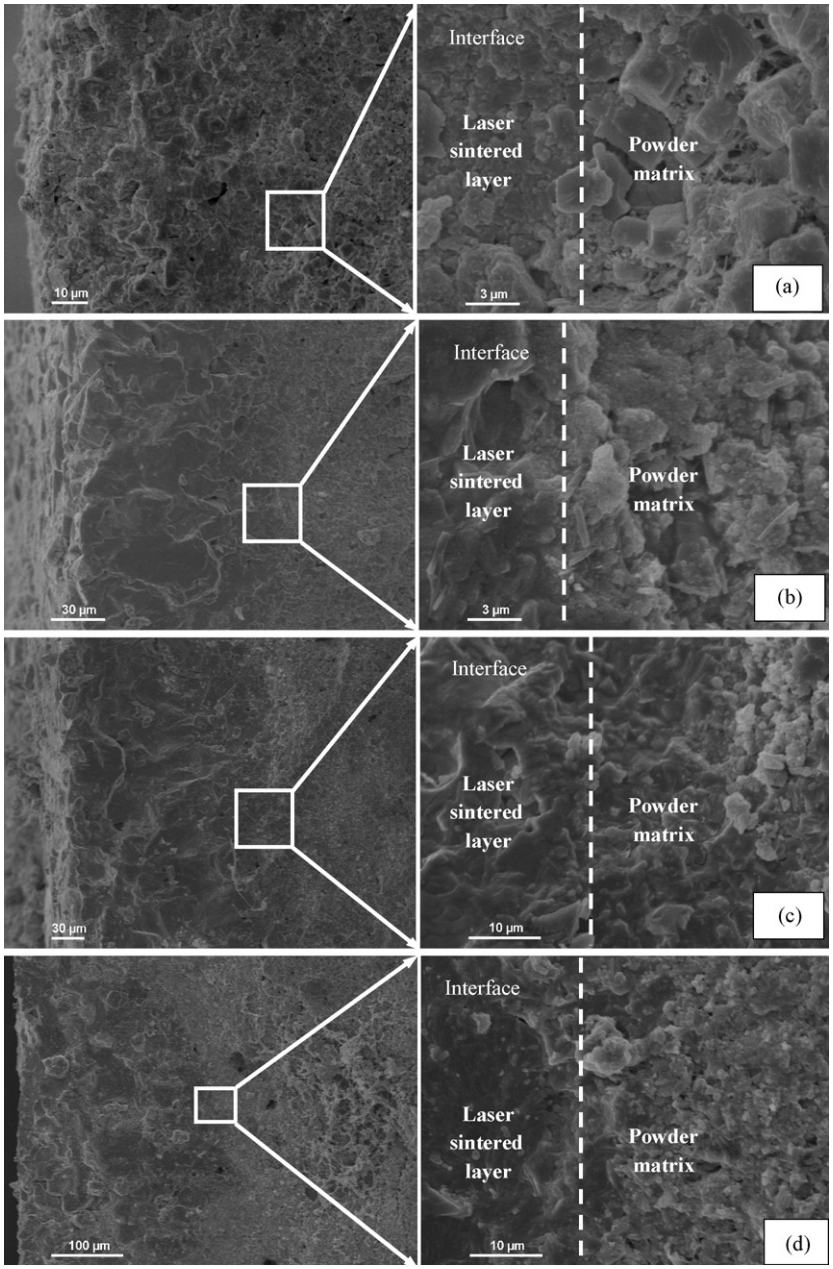

Fig. 5. Microstructural development in the fracture cross-section of KNN samples prepared by laser direct sintering with different laser power: (a) 25 W, (b) 37.5 W, (c) 45 W, and (d) 55 W; the same scan speed of 100 mm/s and hatching space of 0.1 mm.

samples had more than ten times bigger *F* values than the furnace sintered one. The maximum *F* value of 38.5% has been achieved at the laser power level of 55 W. This value is higher than the result of 23% provided by Ji et al. [24] even though a needle-like microstructure had been attained in their research. But it is still much lower than the *F* value of 95% of the specimens prepared by the reactive templated grain growth [30]. Although textured structure has been confirmed to be beneficial to the physical properties only by laser direct sintering without adding any orientated templates [24], further piezoelectric properties measurement should be still carefully conducted in the following works.

Volatilization of alkali metal oxide always happens in the conventional KNN sintering process, which causes the difficulty of fabricating high-density ceramics with good piezoelectric properties. Even using the laser sintering process, Ji et al. still utilized O_2 discharged around the irradiated samples through a coaxial nozzle to suppress the evaporation of Na_2O [24]. In the present research, chemical composition has been detected by using XRF analysis. As shown in Table 1, the Na_2O content decreased almost 2.5% from 30.22% in the starting KNN powder when subjected to the laser irradiation. But the increasing laser power did not improve the evaporation of Na_2O. These results were attained by using the pow-

Table 1
XRF analysis results for the laser sintered KNN samples with different laser power.

Laser power (W)	Chemical composition (mol%)		
	K_2O	Na_2O	Nb_2O_5
0[a]	23.01	30.22	46.77
25	26.13	27.72	46.15
37.5	26.12	27.73	46.15
45	26.49	27.87	45.64
55	25.91	27.9	46.19

[a] Starting powder without laser sintering.

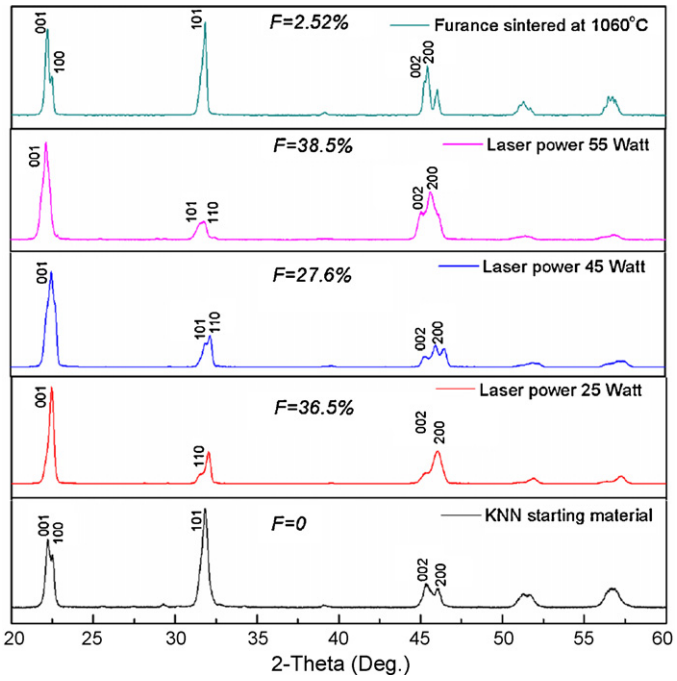

Fig. 6. XRD patterns and Lotgering *F* values of KNN samples prepared by different processes.

der XRF analysis. In order to get these XRF results the laser sintered KNN specimens must be firstly ground into powder. However it was very difficult to completely separate the laser sintered layer from the powder matrix. In this process, unsintered KNN powder was inevitably mixed into the testing sample. So these XRF results might be not significant enough to confirm the influence of different laser power on the evaporation of Na_2O. Surface and cross-section μ-XRF analyses are underway right now. Anyway, volatilization of Na_2O had been confirmed. Some measures should be taken to suppress the evaporation or compensate the content of Na_2O in the final KNN products.

4. Conclusions and outlook

In order to utilize KNN ceramics for the fabrication of 3D ceramic components by using the layer-wise laser direct sintering process, the laser sinterability of KNN powder has been investigated according to the SEM, XRD, and XRF analyses. Some conclusions can be made as follows:

1. Laser sintered thickness can be controlled by adjusting the laser power. Microstructures of the laser sintered KNN samples are similar to the conventional sintered ones. Cubic grains have been observed in the laser sintered KNN specimens. The size of cubic grains can also be controlled by adjusting the laser power.
2. XRD results confirmed that the pure perovskite KNN phases and textured structures can be attained by using laser as the heat source. These textured structures are expected to improve the piezoelectric properties of the final KNN components.
3. KNN ceramics can be sintered by laser and be utilized in the layer-wise laser direct sintering process to produce 3D components.

In the future work, the relationship between laser sintering parameters and the morphologies (grain size, orientation degree, and evaporation of alkali metal oxide) as well as the piezoelectric properties should be investigated. Water based KNN slurries should be prepared for the following rapid manufacturing process.

Acknowledgements

The authors are deeply indebted to Mr. Görke for the SEM analysis, Mrs. Ohlendorf for machining the samples and Mr. Zellmann for the XRD and XRF analyses.

References

[1] Y. Saito, H. Takao, T. Tani, T. Nonoyama, K. Takatori, T. Homma, T. Nagaya, M. Nkakmura, Nature (London) 42 (2004) 84.
[2] L. Egerton, D.M. Dillon, J. Am. Ceram. Soc. 42 (1959) 438.
[3] R.E. Jaeger, L. Egerton, J. Am. Ceram. Soc. 45 (1962) 209.
[4] J. Li, K. Wang, B. Zhang, L. Zhang, J. Am. Ceram. Soc. 89 (2006) 706.
[5] Y. Guo, K. Kakimoto, H. Ohsato, Appl. Phys. Lett. 85 (2004) 4121.
[6] M. Matsubara, T. Yamaguchi, K. Kikuta, S. Hirano, Jpn. J. Appl. Phys. 43 (2004) 7159.
[7] D. Lin, K.W. Kwork, K.H. Lam, H.L.W. Chan, J. Phys. D: Appl. Phys. 40 (2007) 3500.
[8] B. Malic, J. Bernard, J. Holc, D. Jenko, M. Kosec, J. Eur. Ceram. Soc. 25 (2005) 2707.
[9] T. Saito, T. Wada, H. Adachi, I. Kanno, Jpn. J. Appl. Phys. 43 (2004) 6627.
[10] C. Cho, A. Grishin, Appl. Phys. Lett. 75 (1999) 268.
[11] M. Blomqvist, J. Koh, S. Khartsev, A. Grishin, J. Andreasson, Appl. Phys. Lett. 81 (2002) 337.
[12] H. Lee, I. Kim, J. Kim, C. Ahn, B. Park, Appl. Phys. Lett. 94 (2009) 092902.
[13] C. Ahn, E. Jeong, S. Lee, H. Lee, S. Kang, I. Kim, Appl. Phys. Lett. 93 (2008) 212905.
[14] J. Ryu, J. Choi, B. Hahn, D. Park, W. Yoon, K. Kim, Appl. Phys. Lett. 90 (2007) 152901.
[15] T. Kimura, J. Ceram. Soc. Jpn. 114 (2006) 15.
[16] N.M. Hagh, K. Nonaka, M. Allahverdi, A. Safari, J. Am. Ceram. Soc. 88 (2005) 3043.
[17] Y. Zhen, J. Li, J. Am. Ceram. Soc. 90 (2007) 3496.
[18] A. Bacciochini, N. Glandut, P. Lefort, J. Eur. Ceram. Soc. 29 (2009) 1507.
[19] L. Sartinska, S. Barchikovski, N. Wagenda, B. Rud, I. Timofeeva, Appl. Surf. Sci. 253 (2007) 4295.
[20] L. Bradley, L. Li, F. Stott, Appl. Surf. Sci. 138–139 (1999) 233.
[21] Y. Wu, J. Du, K. Choy, L. Hench, J. Eur. Ceram. Soc. 27 (2007) 4727.
[22] S. Harimkar, N. Dahotre, J. Appl. Phys. 100 (2006) 024901.
[23] S. Harimkar, N. Dahotre, Phys. Stat. Sol. (a) 204 (2007) 1105.
[24] L. Ji, Y. Jiang, Y. Gao, X. Du, J. Laser Appl. 21 (2009) 124.
[25] L. Ji, Y. Jiang, W. Wang, Z. Yu, Appl. Phys. Lett. 85 (2004) 1577.
[26] Z. Macedo, M. Lente, J. Eiras, A. Hernandes, J. Phys.: Condens. Matter 16 (2004) 2811.
[27] X. Tian, B. Sun, J. Heinrich, D. Li, Mater. Sci. Eng. A 527 (2010) 1695.
[28] X. Tian, J. Günster, J. Melcher, J. Heinrich, D. Li, J. Eur. Ceram. Soc. 29 (2009) 1903.
[29] C. Ahn, C. Park, C. Choi, S. Nahm, M. Yoo, H. Lee, J. Am. Ceram. Soc. 92 (2009) 2033.
[30] H. Takao, Y. Saito, Y. Aoki, K. Horibuchi, J. Am. Ceram. Soc. 89 (2006) 1951.
[31] B. Zhang, J. Li, K. Wang, H. Zhang, J. Am. Ceram. Soc. 89 (2006) 1605.
[32] R. Zuo, J. Roedel, R. Chen, L. Li, J. Am. Ceram. Soc. 89 (2006) 2010.
[33] H. Song, K. Cho, H. Park, C. Ahn, S. Nahn, K. Uchino, S. Park, H. Lee, J. Am. Ceram. Soc. 90 (2007) 1812.
[34] F. Lotgering, J. Inorg. Nucl. Chem. 9 (1959) 113.